

Synthesis, Optical Properties and Photovoltaic Application of the SnS Quasi-one-dimensional Nanostructures

M. X. Wang^{1,2}, G. H. Yue^{1,*}, Y. D. Lin¹, X. Wen¹, D. L. Peng¹, Z. R. Geng³

(Received 25 October 2012; accepted 14 December 2012; published online 30 January 2013)

Abstract: Low-toxicity single crystal SnS nanowires had been successfully synthesized by the catalyst-assistant chemical vapor deposition. Au nanoparticles were applied on the ITO surface as the catalysis, using SnS powder and S powder as forerunners. The structure, morphology and optical properties of the prepared SnS nanowires were characterized. The experimental results show the as-synthesized nanowires are single crystalline with a preferential orientation. The synthesized SnS nanowires show strong absorption in the visible and near-infrared spectral region, and the direct energy band gap of SnS nanowires is 1.46 eV.

Keywords: Nanostructure; Chemical vapor deposition; Crystal growth; Optical property

Citation: M. X. Wang, G. H. Yue, Y. D. Lin, X. Wen, D. L. Peng and Z. R. Geng, "Synthesis, Optical Properties and Photovoltaic Application of the SnS Quasi-one-dimensional Nanostructures", *Nano-Micro Lett.* 5(1), 1-6 (2013). <http://dx.doi.org/10.3786/nml.v5i1.p1-6>

Introduction

In the last several years, as one of the most important candidate materials for the solar cell, SnS has attracted much attention and recognition [1-8]. Firstly, SnS is an environment-friendly material without toxic. Secondly, the electrical conductivity of the SnS can be easily controlled by doping with others. Thirdly, the photoelectric conversion efficiency of the SnS material is very high than others, and the optical energy band gap of the SnS is suitable for the solar cell. Fourthly, the optical absorption coefficient of SnS is very large. For all of these reasons, SnS is one of the most important candidate materials for the solar cell. And yet, the solar cell's efficiency has to be increased and the costs have to be reduced simultaneously. Nanowire is a promising material system to realize this. Due to the small size of nanowires, different materials can

be more easily combined compared with bulk systems, and more sophisticated tandem cells could be fabricated. Secondly, the nanowires with long absorption path lengths maintain short distances for carrier collection/transportation. Thirdly, strong light trapping occurred in high-density nanowire arrays. At last, the cost of nanowire solar cells may be reduced by using cheaper fabrication methods by the fact that less of the rare metals are being used in these nanostructured.

Crystalline tin sulfides have been prepared by various methods and most of the properties had been studied [9-12]. To our knowledge, most of them are thin films or nanoparticles, only a little report about preparing novel quasi-one-dimensional wire-like SnS nanostructures. Single crystalline SnS nanowires were synthesized using solution methods [13]. Nanorods and nanosheets of SnS were synthesized by a novel thioglycolic acid assisted hydrothermal process [14]. SnS

¹Department of Materials Science and Engineering, Fujian Key Laboratory of Advanced Materials, Xiamen University, Xiamen 361005, China

²Department of Materials Engineering, Lanzhou Institute of Technology, Lanzhou 730050, China

³School of Mechatronic Engineering, Lanzhou Jiao Tong University, Lanzhou, 730070, China

*Corresponding author. E-mail: yuegh@126.com

nanowires grown on tin foils were synthesized using surfactant-assisted process and the growth mechanism had been discussed also by S. K. Panda [15]. Superior rate capabilities of SnS nanosheet electrodes for Li ion batteries had been reported in 2010 [16]. Using the template-assisted pulsed electrochemical deposition, our group had successfully synthesized the SnS nanowire arrays, and the optical properties of the synthesized SnS nanowires had also been discussed [17].

In this paper, we present a simple method of producing single crystal SnS nanowires by a simple chemical vapor deposition method. Nanostructure and optical properties of the as-synthesized SnS nanomaterials have been studied. And with this method, the aligned SnS nanowire arrays can be synthesized easily with short reaction time or lower reaction rate.

Experimental

A conventional horizontal tube furnace was used for the synthesis. A quartz tube with an inner diameter of 30 mm, and length of 900 mm was installed in the furnace. Another alumina tube with an inner diameter of 20 mm, and length of 600 mm was inserted into the quartz tube. Sulfur (2 g), SnS (2 g) and the substrate were loaded in the alumina tube in turn, where the distance between the SnS powder and substrate was about 10 cm, and the distance between the sulfur powder and SnS powder was about 5 cm. The indium tin oxide (ITO) glass substrates were cleaned in diluted HF solution for 30 s then rinsed with deionized water. Several drops of water-dispersed colloidal Au nanoparticles with a nominal diameter of 10 nm were applied to the ITO surface with a similar amount of dilute HF solution, and left dormant for 30 s. After being rinsed with deionized water, the substrates were dried by a nitrogen gun and placed onto the CVD system.

After the quartz tube was evacuated by a vacuum system to about 10^{-3} Pa, the tube was backfilled with a high-purity carrier gas of Ar, and then the temperature of the furnace central region was increased with a rate of $50^{\circ}\text{C}/\text{min}$. The temperature of the central region of the furnace was kept for 30 min within an operating temperature (750°C and 790°C), and keep the nanowires growth region no more than 300°C , during which the Ar flow rate was 200 sccm (standard-state cubic centimeter per minute), and at the same time a small hydrogen flow (10 sccm) was introduced into the system. And the temperature of the sulfur region was about 150°C . Afterwards, the furnace was left to naturally cooling down to room temperature. After deposition, the substrate was covered with black product. These products were characterized by X-ray diffraction (XRD), field-emission scanning electron microscopy (FE-SEM), high resolution transmission electron microscopy (HRTEM). Energy dispersive X-ray spectroscopy (EDS) attaching

to FE-SEM was used to analyze the elemental composition of the samples. In order to get the optical characterization of all deposited films, transmission and reflectance spectra measurements at room temperature were measured with a Shimadzu model 3101PC double-beam spectrophotometer. The absorption coefficient (α) was calculated from $T(\lambda)$ and $R(\lambda)$ measurements, as well, its dependence on the photon energy ($h\nu$) and the optical band gap (E_g) was obtained. Photovoltaic measurements were recorded by a Keithley 2400 digital source meter. Solar cell performance was measured by utilizing an Air Mass 1.5 G (AM1.5 G) solar simulator with an irradiation intensity of $100\text{ mW}/\text{cm}^2$ under ambient conditions.

Results and Discussion

Figure 1 shows a series of SEM and TEM images of as-grown quasi-one-dimensional SnS nanostructures. Figure 1(a-d) is the SEM images of SnS nanostructures deposited on gold particles-filled ITO substrate. The sample in Fig. 1(a) grew at 790°C for 30 min with the Ar and H_2 flow rates of 200 sccm and 10 sccm, respectively. SEM observation reveals that this sample consists of large amount of curly and uniform SnS nanowires. Figure 1(b) was the high magnification image of the Fig. 1(a), it can be found that the nanowires are uniformly with a diameter of 50 nm and length of several micrometers. The sample in Fig. 1(c) grew at 750°C for 30 min with 200 sccm Ar and 10 sccm H_2 , and Fig. 1(d) was the high magnification image of the Fig. 1(c). From the Fig. 1(c) and Fig. 1(d), it can be found that the nanowires are messily piled up and the diameter of the nanowires changed from 10 nm to 100 nm, as the reaction temperature was 750°C . When the reaction temperature changes to 700°C , there appears the nanobelts and the comb-like nanostructure. This kind of phenomenon has appeared in our work with the ZnO nanostructure [18]. The nanostructures of the sample which grew at 790°C for 30 min with the Ar and H_2 flow rates of 200 sccm and 10 sccm were further studied by TEM and found to be nanowires. In Fig. 1(e), the inset is the selected area electron diffraction (SAED) pattern of the nanowires, which indicates the nanowire is single crystalline orthorhombic SnS in structure. HRTEM was used for further insight into the structure of the nanowires. Figure 1(f) is obtained from HRTEM recorded on an individual nanowire and which is acquired by enlargement of a selected area of a single nanowire from the Fig. 1(e). It is indicated that the SnS nanowire sample exhibits good crystalline and continuous lattice fringes over a larger area. This image clearly reveals that the as-synthesized nanowire has no obvious defect of dislocation. The interplanar spacing is 0.293 nm, which corresponds to the $d(101)$ spacing for the orthorhombic structure, confirming the

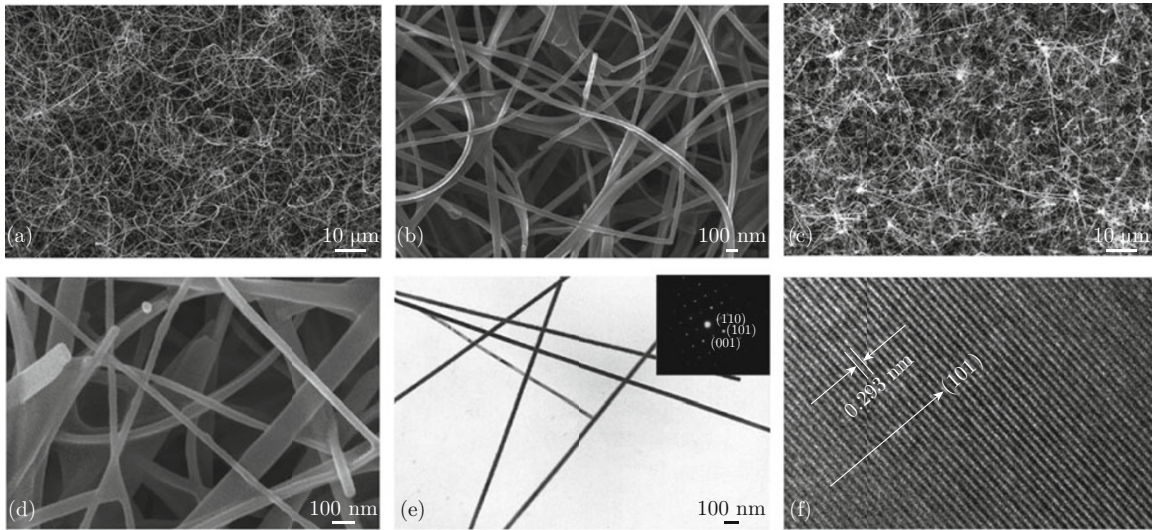


Fig. 1 SEM images of SnS nanostructures grown on Au particles covered ITO substrates at 790°C (a-b) and 750°C (c-d), respectively. (e) and (f) are TEM images corresponding to the sample in (a). And the inset in (e) is the selected area electron diffraction pattern of the nanowires. (Note: The samples were checked after the Au nanoparticles had been removed.)

crystalline nature of the produced SnS nanowires [16]. EDS attached to SEM was used to investigate the chemical composition of the products. The molar ratio of Sn and S in the sample is 48.15 and 51.85, respectively. Therefore, the tin atom quantity is insufficient in the as-synthesized SnS nanowires.

XRD analysis shows that all the samples are orthorhombic SnS with lattice parameters of $a = 4.36 \text{ \AA}$, $b = 11.09 \text{ \AA}$ and $c = 3.98 \text{ \AA}$. Figure 2 shows the presentative XRD patterns of the as-prepared samples grown at 790°C for 30 min with the Ar and H₂ flow rates of 200 sccm and 10 sccm, in which all the peaks are indexed to orthorhombic SnS. From Fig. 2, it can be seen that the major peak (101) is strongly dominating other peaks indicating the preferred orientation. No impurities such as SnO₂ and SnS₂ can be detected from the XRD analysis. The sharp and narrow (101)

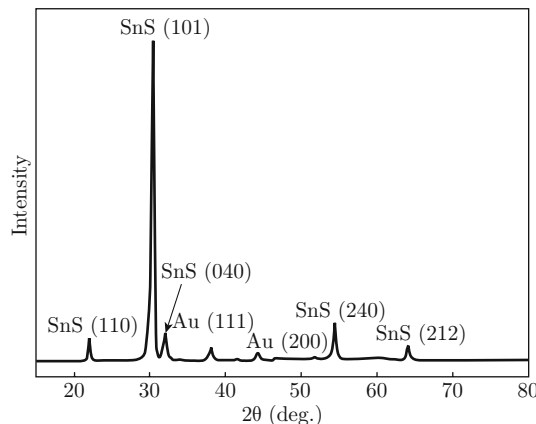


Fig. 2 XRD patterns of the as-prepared SnS nanostructures corresponding to the samples in Fig. 1(a). (Note: The samples were checked before the Au nanoparticles had been removed.)

peaks indicate that the nanowires are highly crystalline and consist of only a single compositional phase, and this is corresponding to the HRTEM and SAED results. And the growth mechanism (VLS) had been discussed in our earlier work. [19]

In order to determine optic properties of the as prepared SnS nanowires, the optic transmission (T) spectrum measurements at room temperature were taken in the wavelength range of 350–1100 nm. The optic transmission spectra of the samples growing at 790°C for 30 min with the Ar and H₂ flow rates of 200 sccm and 10 sccm are shown in Fig. 3. It is seen from the Fig. 3 (see the dotted lines) that the transmission of the samples is very low when the wavelength is in the range of 350–550 nm, and then the $T(\%)$ increases with the wavelength increasing. The variation of reflection (R) spectra of the same samples as a function of wavelengths are shown in Fig. 3 as well (see the solid line). It is considered that the $R(\%)$ is about 35% when the wavelength is no more than 500 nm and it also decreased rapidly first and then slowly when the wavelength is more than 1000 nm. It was well known that the transmission T through an absorbing slab is related to its reflectivity R , thickness d , and absorption α by [17, 20]

$$T = (1 - R) \cdot e^{-\alpha d} \quad (1)$$

Or

$$\alpha = \frac{1}{d} \ln \left[\frac{(1 - R)^2 + \sqrt{(1 - R)^4 + (2RT)^2}}{2T} \right] \quad (2)$$

Herein the thickness d of the nanowires films is about 10 μm for the SnS nanowires films. Therefore, the absorption coefficient α can be calculated from the data of $T(\lambda)$ and $R(\lambda)$. It was found that the optic absorption coefficient calculated for SnS nanowires was higher

than 10^5 cm^{-1} in the wavelength range from 400 nm to 800 nm (See Fig. 4(a)).

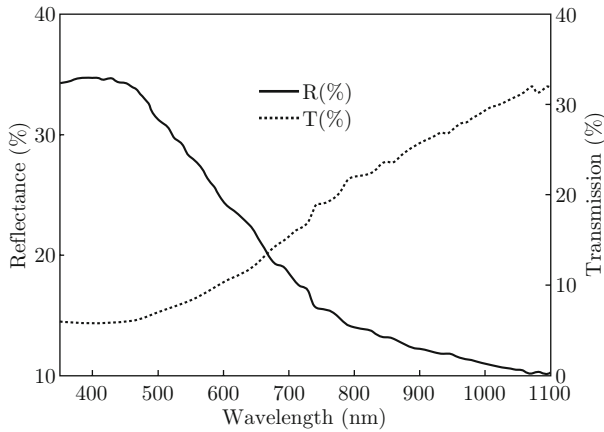


Fig. 3 Transmission spectra and reflectance spectra as a function of wavelength for the as-prepared SnS nanowires which grown at 790°C for 30 min with the Ar and H_2 flow rates of 200 sccm and 10 sccm, respectively. (Note: The samples were checked after the Au nanoparticles had been removed.)

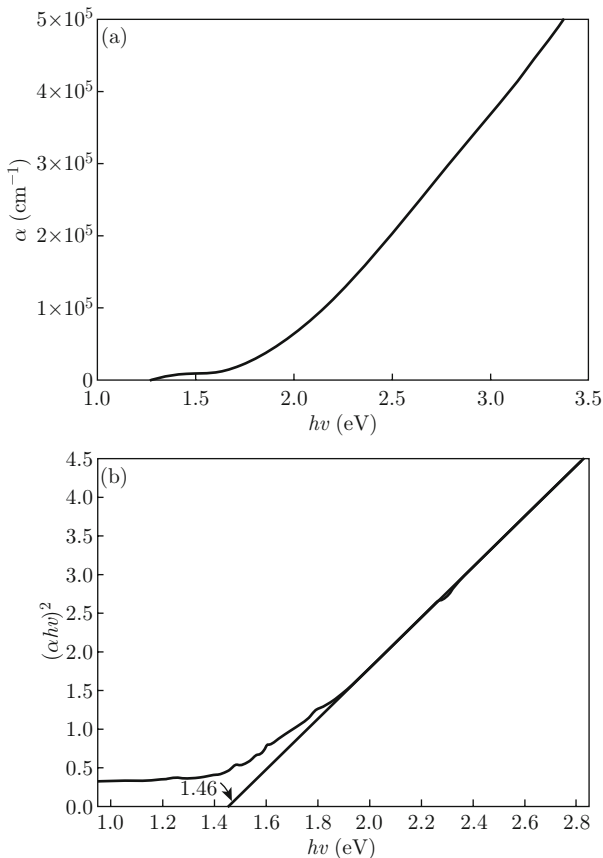


Fig. 4 (a) is the dependence of absorption coefficient on photon energy and (b) is the plots of $(\alpha hv)^2$ vs. (hv) for the SnS nanowires which grew at 790°C for 30 min with the Ar and H_2 flow rates of 200 sccm and 10 sccm, respectively. (Note: The samples were checked after the Au nanoparticles had been removed.)

To determine the energy band gap, E_g , and the type of optical transition responsible for this intense optical absorption, the absorption spectrum was analyzed using the equation for the near-edge absorption [2,6,17].

$$(\alpha hv)^n = A(hv - E_g) \quad (3)$$

Where A is a constant and n characterizes the transition process. We can see $n=2$ and $2/3$ for direct allowed and forbidden transitions, respectively, and $n=1/2$ and $1/3$ for indirect allowed and forbidden transitions, respectively.

Figure 4(b) shows curves of $(\alpha hv)^2$ versus hv of the SnS nanowires. The straight line had been made a good fit with the curve in the higher energy range above the absorption edge, which indicates a direct optical transition near the absorption edge. From Fig. 4, the direct energy gap E_g of the sample has been calculated as 1.46 eV, which is higher than the value of SnS bulk or film. The nanowires' diameter 50 nm is far greater than the Bohr radius, therefore, and it can be suggested the increased band gap values do not exhibit quantum size effects [17,21,22]. The energy band gap at 1.46 eV detected in our study may be attributed to the surface effect of the carriers in the semiconductor nanowires. The lattice distortion inducing a smaller lattice constant or surface lattice defects will lead to a size dependent enlargement of the band gap, which results in a blue shift for the absorbance onset, as observed in this work.

In order to study the photovoltaic behavior, a grating Al electrode about 200 nm was evaporated on the SnS nanowires film. The current-voltage (I - V) characteristics of the SnS nanowires sandwiched between ITO and Al contacts, in the dark and under 100 mW/cm^2 AM1.5 solar illuminations are shown in Fig. 5. These measurements show that the SnS nanowires act as photoconductors. There is negligible photovoltaic behavior,

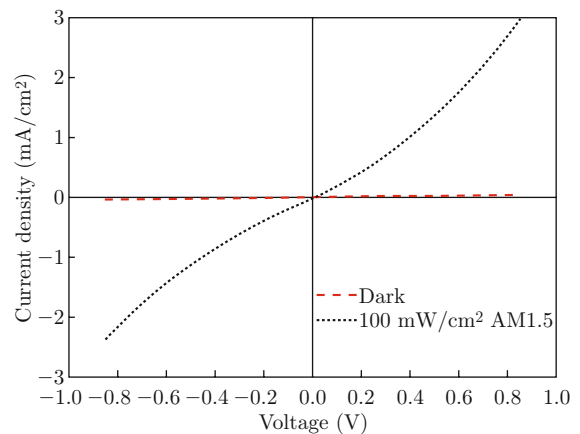


Fig. 5 The current-voltage (I - V) characteristics of the SnS nanowires sandwiched between ITO and Al contacts. (Note: The samples were checked after the Au nanoparticles had been removed.)

indicating the absence of any significant Schottky barrier formed at the nanowires/electrode interface. This result indicated that the rectifying behavior was not coming from the interface contacts, or the rectifying behavior between the nanowires/electrode interfaces is very weak and can be ignored. So, the p-n junction photovoltaic cells with homojunction or heterojunction are ongoing.

Conclusion

The low-toxicity SnS nanowire arrays have been successfully synthesized using the catalyst-assistant chemical vapor deposition methods. SEM and FE-SEM results indicated the diameter and morphology changed with the preparation conditions. And the best condition to obtain nanowire is keeping the reaction temperature at 790°C. With the temperature decreasing, two dimensional nanostructure would appeared. The as-prepared SnS nanowires have a diameter of about 50 nm and length up to several micrometer or longer. The SAED shows the product is a single crystalline structure. The XRD pattern indicates the nanowires are composed of SnS phase and have a highly preferential (101) orientation. According to the transmission spectra and the reflection spectra, we can calculate the properties of synthesized SnS nanowires which exhibit strong absorption in the visible and near-infrared spectral region. The direct energy gap E_g of the SnS nanowires has been calculated as 1.46 eV, and the experimental optical band gap value is the evidence for the lattice distortion of the SnS nanowires. Other properties of the SnS nanowires will be coming up and the SnS combined nanodevice will be studied rapidly. The current-voltage (I - V) characteristics of the SnS nanowires sandwiched between ITO and Al contacts have also been studied.

Acknowledgements

This work was partially supported by the National Science Foundation of China (No. 50902117, No. 11104126 and No. 50825101), the Natural Science Foundation of Fujian Province of China (Grant No. 2009J01263) and the National Basic Research Program of China (No. 2012CB933103), and Scientific and Technological Innovation Platform of Fujian Province (2006L2003).

References

- [1] N. K. Reddy, Y. B. Hahn, M. Devika, H. R. Sumana and K. R. Gunasekhar, "Temperature-dependent structural and optical properties of SnS films", *J. Appl. Phys.* 101, 093522-093528 (2007). <http://dx.doi.org/10.1063/1.2729450>
- [2] G. H. Yue, D. L. Peng and P. X. Yan, "Structure and optical properties of SnS thin film prepared by pulse electrodeposition", *J. Alloys Compd.* 468(1-2), 254-257 (2009). <http://dx.doi.org/10.1016/j.jallcom.2008.01.047>
- [3] C. W. Wolfe, "Physical properties of semiconductors", Prentice-Hall, Englewood Cliffs, NJ (1989).
- [4] M. Devika, N. K. Reddy and K. Ramesh, "Low resistive micrometer-thick SnS: Ag films for optoelectronic applications", *J. Electrochem. Soc.* 153(8), G727-G733 (2006). <http://dx.doi.org/10.1149/1.2204870>
- [5] A. Ghazali, Z. Zainal, M. Z. Hussein and A. Kassim, "Cathodic electrodeposition of SnS in the presence of EDTA in aqueous media", *Sol. Energ. Mat. Sol. C.* 55(3), 237-249 (1998). [http://dx.doi.org/10.1016/S0927-0248\(98\)00106-8](http://dx.doi.org/10.1016/S0927-0248(98)00106-8)
- [6] G. H. Yue and W. Wang, "The effect of anneal temperature on physical properties of SnS films", *J. Alloy. Compd.* 474(1-2), 445-449 (2009). <http://dx.doi.org/10.1016/j.jallcom.2008.06.105>
- [7] M. Parenteau and C. Carlone, "Influence of temperature and pressure on the electronic transitions in SnS and SnSe semiconductors", *Phys. Rev. B* 41(8), 5227-5234 (1990). <http://dx.doi.org/10.1103/PhysRevB.41.5227>
- [8] B. Subramanian, C. Sanjeeviraja and M. Jayachandran, "Photoelectrochemical characteristics of brush plated tin sulfide thin films", *Sol. Energ. Mat. Sol. C.* 79(1), 57-65 (2003). [http://dx.doi.org/10.1016/S0927-0248\(02\)00366-5](http://dx.doi.org/10.1016/S0927-0248(02)00366-5)
- [9] B. Thangaraju and P. Kaliannan, "Spray pyrolytic deposition and characterization of SnS and SnS₂ thin films", *J. Phys. D: Appl. Phys.* 33, 1054-1059 (2000). <http://dx.doi.org/10.1088/0022-3727/33/9/304>
- [10] L. S. Price, I. P. Parkin and M. N. Field, "Atmospheric pressure chemical vapour deposition of tin(II) sulfide films on glass substrates from $\text{Bun}_3\text{SnO}_2\text{CCF}_3$ with hydrogen sulfide", *J. Mater. Chem.* 10(2), 527-530 (2000). <http://dx.doi.org/10.1039/a907939d>
- [11] A. Tanusevski, "Optical and photoelectric properties of SnS thin films prepared by chemical bath deposition", *Semicond. Sci. Technol.* 18, 501-505 (2003). <http://dx.doi.org/10.1088/0268-1242/18/6/318>
- [12] D. S. Koktysh, J. R. McBride and S. J. Rosenthal, "Synthesis of SnS nanocrystals by the solvothermal decomposition of a single source precursor", *Nanoscale Res. Lett.* 2, 144-148 (2007). <http://dx.doi.org/10.1007/s11671-007-9045-9>
- [13] Y. K. Liu, D. D. Hou and G. H. Wang, "Synthesis and characterization of SnS nanowires in cetyltrimethylammoniumbromide (CTAB) aqueous solution", *Chem. Phys. Lett.* 379(1-2), 67-73 (2003). <http://dx.doi.org/10.1016/j.cplett.2003.08.014>
- [14] S. Biswas, S. Kar and S. Chaudhuri, "Thioglycolic acid (TGA) assisted hydrothermal synthesis of SnS nanorods and nanosheets", *Appl. Surf. Sci.*

- 253(23), 9259-9266 (2007). <http://dx.doi.org/10.1016/j.apsusc.2007.05.053>
- [15] S. K. Panda, A. Datta, A. Dev, S. Gorai and S. Chaudhuri, "Surfactant-assisted synthesis of SnS nanowires grown on tin foils", *Cryst. Growth Des.* 6(9), 2177-2181 (2006). <http://dx.doi.org/10.1021/cg0602156>
- [16] J. Kang, J. Park and D. Kim, "Superior rate capabilities of SnS nanosheet electrodes for Li ion batteries", *Electrochem. Commun.* 12(2), 307-310 (2010). <http://dx.doi.org/10.1016/j.elecom.2009.12.025>
- [17] G. H. Yue, L. S. Wang, X. Wang, Y. Z. Chen and D. L. Peng, "Characterization and optical properties of the single crystalline SnS nanowire arrays", *Nanoscale Res. Lett.* 4, 359-363 (2009). <http://dx.doi.org/10.1007/s11671-009-9253-6>
- [18] J. Z. Liu, P. X. Yan, G. H. Yue, J. B. Chang, R. F. Zhuo and D. M. Qu, "Controllable synthesis of undoped/Cd-doped ZnO nanostructures", *Mater. Lett.* 60(25-26), 3122-3125 (2006). <http://dx.doi.org/10.1016/j.matlet.2006.02.056>
- [19] G. H. Yue, Y. D. Lin and X. Wen, "Synthesis and characterization of the SnS nanowires via chemical vapor deposition", *Appl. Phys. A Mater. Sci. Process.* 106(1), 87-91 (2012). <http://dx.doi.org/10.1007/s00339-011-6560-4>
- [20] D. Avellaneda, G. Delgado, M. T. S. Nair and P. K. Nair, "Structural and chemical transformations in SnS thin films used in chemically deposited photovoltaic cells", *Thin Solid Films* 515(15), 5771-5776 (2007). <http://dx.doi.org/10.1016/j.tsf.2006.12.078>
- [21] H. Tang, G. Y. Xu, L. Q. Weng, L. J. Pan and L. Wang, "Luminescence and photophysical properties of colloidal ZnS nanoparticles", *Acta Mater.* 52(6), 1489-1494 (2004). <http://dx.doi.org/10.1016/j.actamat.2003.11.030>
- [22] T. Takagahara, "Effects of dielectric confinement and electron-hole exchange interaction on excitonic states in semiconductor quantum dots", *Phys. Rev. B* 47(8), 4569-4584 (1993). <http://dx.doi.org/10.1103/PhysRevB.47.4569>